

Thunderscapes: Simulating the Dynamics of Mesoscale Convective System

Tianchen Hao

Abstract

A Mesoscale Convective System (MCS) is a collection of thunderstorms that function as a system, representing a widely discussed phenomenon in both the natural sciences and visual effects industries, and embodying the untamed forces of nature. In this paper, we present the first interactive, physically inspired mesoscale thunderstorms simulation model that integrates Grabowski-style cloud microphysics with atmospheric electrification processes. Our model simulates thunderclouds development and lightning flashes within a unified meteorological framework, providing a realistic and interactive approach for graphical applications. By incorporating key physical principles, it effectively links cloud formation, electrification, and lightning generation. The simulation also encompasses various thunderstorm types and their corresponding lightning activities.

1 INTRODUCTION

Thunderstorms represent the wild power of nature and are a common atmospheric element in visual effects (VFX) industry. Notable works, such as *Horizon Forbidden West: Burning Shores* and *Ghost of Tsushima* (see Figure ??), demonstrate the importance of realistic atmospheric effects. Modern applications demand tools for efficient and realistic simulation of thunderstorms. However, current general purpose VFX software, such as Houdini and Maya, lacks standardized toolkits specifically designed for creating atmospheric phenomena like thunderstorms. Artists often rely on traditional Eulerian fluid dynamics (e.g., stable fluids [Stam(1999)]) to simulate smoke and manually control the evolution of cloud shapes. Lightning, on the other hand, is typically generated using L-system based methods to create fractional geometries. However, these approaches do not account for the natural dynamics and interrelationship between thunderclouds and lightning.

Recent advances in computer graphics research have increasingly focused on cloud dynamics, incorporating atmospheric microphysical processes [Hädrich et al.(2020), Herrera et al.(2021), Amador Herrera et al.(2024)]. However, the critical role of atmospheric electrification in cloud development remains underexplored. This study aims to address this gap by integrating the electrification process, thus

enhancing the consistency and realism of phenomena observed during thunderstorm events.

This paper presents an interactive, physically inspired method for simulating thunderstorm development. By coupling cloud microphysics with atmospheric hydrometeor electrification, our approach captures essential processes that contribute to the consistent formation of mesoscale thunderstorm phenomena.

The key contributions include:

- (1) We present a comprehensive framework for computing thunderstorm microphysics in the atmosphere, incorporating the transport of cloud hydrometeors and their electrification processes.
- (2) We introduce a lightweight parameterization that enables users to interactively simulate various types of thunderstorms, along with their corresponding lightning effects.
- (3) We validate our simulation using different meteorological datasets to ensure the generation of physically credible and visually accurate atmospheric effects.

2 RELATED WORK

2.1 Simulating Thunderstorms in Computer Graphics

The simulation of atmospheric phenomena such as thunderstorms has been extensively explored through a variety of computational methods. Webanck et al. [Webanck et al.(2018)] proposed a procedural approach for generating cloudscares, while Miyazaki et al. [Miyazaki et al.(2002)] simulated cumulus clouds by coupling computational fluid dynamics (CFD) with fundamental water transport equations. Such methods are also employed in Lagrangian-based particle methods. Ferreira et al. [Ferreira Barbosa et al.(2015)] and Zhang et al. [Zhang et al.(2020)] utilized position-based fluids (PBF) for adaptive cloud simulations. Smoothed Particle Hydrodynamics (SPH) techniques, as demonstrated by Goswami and Neyret [Goswami and Neyret(2017)], focus on real-time simulations of convective clouds. Additionally, Vimont et al. [Vimont et al.(2020)] proposed a hybrid, 2D-layered atmospheric model to simulate mesoscale skyscapes, contributing to a more detailed and interactive representation of large-scale cloud structures.

Some studies have specifically focused on the simulation of volcanic cloud dynamics. Lastic et al. [Lastic et al.(2022)] employed Lagrangian dynamics to simulate volcanic plumes and pyroclastic flows, while Pretorius et al. [Pretorius et al.(2024)] integrated volcanic eruptions with atmospheric simulations to produce coherent skyscapes. In their framework, lightning effects were incorporated, but the electrification process, which is essential for lightning formation, was not considered, resulting in a physically inaccurate simulation..

In the domain of lightning simulation, Reed and Wyvill [Reed and Wyvill(1994)], Kim and Lin [Kim and Lin(2007)], and Yun et al. [Yun et al.(2017)] developed

methods for the efficient development of lightning branches, contributing to a more realistic representation of the method of electrical discharges.

Recently, more sophisticated microphysical schemes from atmospheric science have been incorporated into computer graphics research. Garcia-Dorado et al. [Garcia-Dorado et al.(2017)] and Hädrich et al. [Hädrich et al.(2020)] adopted the classic Kessler warm cloud microphysics scheme [Kessler(1969)] in cloud simulations, which has been instrumental in capturing the dynamics of cloud formation and precipitation. Herrera et al. [Herrera et al.(2021)] extended cloud simulations to include multiphase cloud dynamics, further enhancing the realism of weather phenomena. Amador Herrera et al. [Amador Herrera et al.(2024)] developed a framework to simulate hurricane and tornado dynamics, incorporating turbulent microphysics to model these extreme atmospheric events with greater accuracy.

2.2 Thunderstorm models in atmospheric sciences

Thunderstorm microphysics and electrification have been widely discussed topics in the field of atmospheric science.

Kessler [Kessler(1969)] proposed a fundamental framework for the distribution and continuity of water substance in atmospheric circulations, which remains influential in the parameterization of the microphysics of warm clouds.

One notable development in cloud microphysics is the work by Grabowski [Grabowski(1998)], who introduced an extended warm cloud microphysics scheme for large-scale tropical circulations. His method divides the parameterization of warm and cold clouds using a temperature interpolation scheme, a significant inspiration for our approach.

In terms of thunderstorm electrification, Solomon et al. [Solomon et al.(2005)] introduced a 1.5-dimensional explicit microphysics thunderstorm model that incorporates a lightning parameterization, addressing key aspects of thunderstorm electrification. Furthermore, Mansell et al. [Mansell et al.(2002)] simulated three-dimensional branched lightning in a numerical thunderstorm model, providing insights on the complex activities of lightning formation. Barthe and Pinty [Barthe and Pinty(2007)] further advanced the field by simulating a supercell storm using a three-dimensional mesoscale model with an explicit lightning flash scheme, capturing the lightning activities specific to supercell thunderstorms. Mansell et al. [Mansell et al.(2010)] also examined the electrification of small thunderstorms using a two-moment bulk microphysics scheme, extending the understanding of lightning activity in small multicell thunderstorms.

Recent studies have focused on exploring the relationship between thundercloud structures and electrification processes. Formenton et al. [Formenton et al.(2013)] used a cloud electrification model to study the relationship between lightning activity and cloud microphysical structure, providing valuable insights into the interaction between cloud formation and lightning generation. More recently, Wu et al. [Wu et al.(2023)] employed coherent Doppler wind lidar to detect and analyze thundercloud structures, offering a novel method for observing thunderstorm activities.

These contributions highlight the ongoing efforts to simulate and understand thunderstorm activities, including cloud microphysics, lightning activity, and the complex interactions between these phenomena.

Our work focuses on the interactive simulation of common thunderstorm types, based on the standard categories in Mesoscale Convective Systems (MCS). According to the National Severe Storms Laboratory (NSSL)¹, these types include single cell, multi-cell, squall line, and supercell thunderstorms. Additionally, our simulation includes common phenomena generated by thundercloud electrification, such as cloud-to-ground (CG) and intra-cloud (IC) lightning².

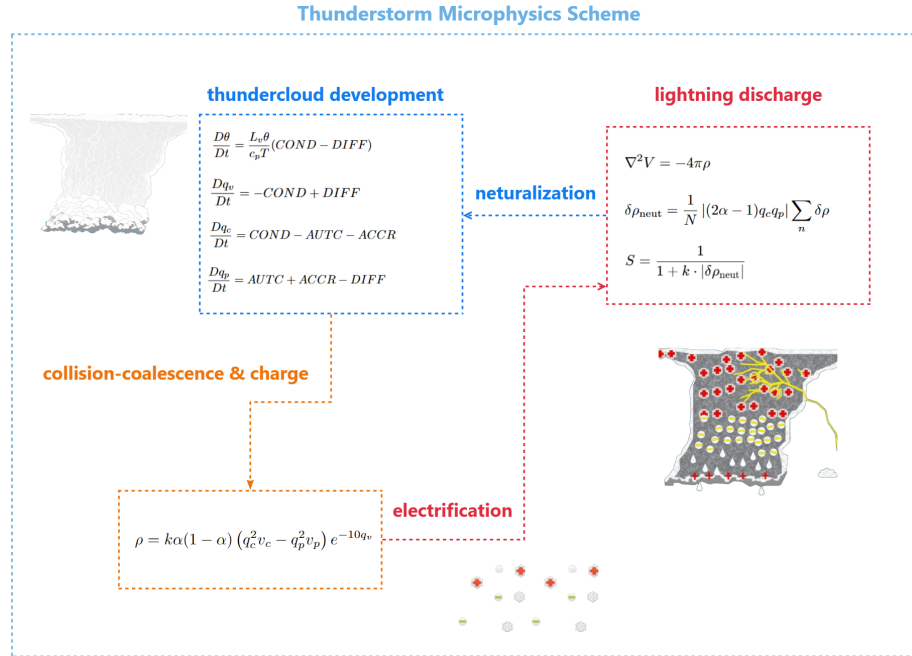


Figure 1: Schematic illustration of our thunderstorm microphysics scheme for hydrometeor phase transitions and the electrification process. The details will be further discussed in Chapter 4. **(I)** Blue frame: the transport of water substances during thundercloud development; **(II)** Orange frame: the accumulation of charge density due to the collision-coalescence of hydrometeors; **(III)** Red frame: the static charge, once it exceeds a given electric field threshold, triggers the lightning discharge process; **(IV)** Blue arrow: the neutralization of hydrometeors following the lightning flash.

¹<https://www.nssl.noaa.gov/education/svrwx101/thunderstorms/types/>

²<https://www.nssl.noaa.gov/education/svrwx101/lightning/types/>

3 OVERVIEW

The primary motivation of our approach is to create consistent atmospheric phenomena during thunderstorms, particularly focusing on thundercloud development and dissipation, along with lightning flashes resulting from the thundercloud electrification processes, as illustrated in Figure 1. By simulating both the microphysics of thunderstorms and their electrodynamic properties, we aim to achieve realistic, interactive weather simulations suitable for graphical applications.

Our model integrates key physical principles to simulate thunderstorm behavior at a mesoscale level. The thunderstorm microphysics component models atmospheric dynamics by coupling a Grabowski-style extended warm cloud microphysics scheme with hydrometeor electrification processing. This approach ensures that the microphysical processes driving cloud formation and growth are consistently linked to the electrification necessary for lightning generation. Additionally, we utilize the compact Poisson filter in our fluid dynamics algorithm to create an efficient simulation of the interactions between cloud particles and atmospheric forces. The compact Poisson filter provides an optimized balance between spectral and iterative methods, enabling high-performance simulations while maintaining stability and accuracy, which is essential for interactive graphics applications.

The key atmospheric quantities driving our model include vapor, cloud water, ice, precipitated rain, precipitated snow, static charge (electric charge distribution within the thundercloud, crucial for lightning formation), and lightning (the flash itself, including both its onset and development).

The simulation is capable of modeling various thundercloud types, including single-cell (a simple, isolated thunderstorm cell), multicell (a cluster of thunderstorm cells with varying stages of development), squall line (a collection of storms that form a line hundreds of miles long, often characterized by a shelf cloud feature), supercell (a large, rotating thunderstorm with the potential to produce tornadoes), and atmospheric river (a narrow corridor of concentrated moisture that can fuel intense thunderstorms).

The lightning types simulated in our model include cloud-to-ground lightning (lightning that strikes from the cloud to the ground) and intra-cloud lightning (lightning occurring between different parts of the same cloud). For the simulation of lightning channel growth, we utilize the Dielectric Breakdown Model (DBM) [Kim and Lin(2007)], which captures the electrodynamics involved in the development of lightning.

The validation of our model is performed by comparing simulated results with real-world weather data. This includes cloud fraction profiles to assess cloud formation and structure, temperature, cloud coverage, and relative humidity evolution compared with real-time weather data from national weather services³, and lightning flash rate over time, evaluated against observed lightning activity.

³<https://www.visualcrossing.com/weather/weather-data-services/>

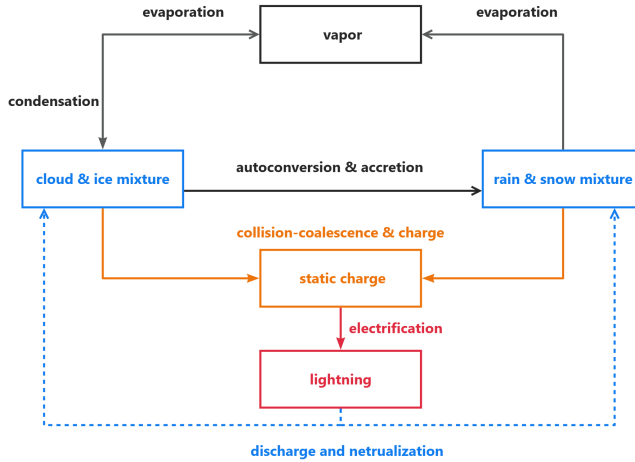


Figure 2: Illustration of our thunderstorm microphysics scheme, which integrates the Grabowski-style extended warm cloud microphysics with the hydrometeor electrification process.

4 METHODOLOGY

Our microphysics model, shown in Figure 2, illustrates the interactions among hydrometeor phase transitions and the electrification mechanisms that lead to lightning. Key processes include the condensation of water vapor into droplets and ice crystals, which subsequently form precipitation through autoconversion and accretion. Evaporation recycles hydrometeors back into the vapor phase, while collisions and coalescence facilitate charge separation. Lightning occurs when the electric field strength exceeds a critical threshold, resulting in the discharge and redistribution of accumulated charge. This feedback loop provides a conceptual framework for understanding thunderstorm development within a mesoscale convective system.

4.1 Cloud Microphysics

The fundamental warm-cloud microphysics equations describe the evolution of potential temperature, water vapor, cloud condensate, and precipitation:

$$\frac{D\theta}{Dt} = \frac{L_v\theta}{c_p T} (COND - DIFF) \quad (1)$$

$$\frac{Dq_v}{Dt} = -COND + DIFF \quad (2)$$

$$\frac{Dq_c}{Dt} = COND - AUTC - ACCR \quad (3)$$

$$\frac{Dq_p}{Dt} = AUTC + ACCR - DIFF \quad (4)$$

Here, θ represents potential temperature, L_v is the latent heat of condensation or evaporation, and c_p is the specific heat capacity at constant pressure. The variables q_v , q_c , and q_p denote the mixing ratios of water vapor, cloud condensate, and precipitation, respectively. The terms $COND$, $DIFF$, $AUTC$, and $ACCR$ represent the condensation rate, diffusional growth rate of precipitation, autoconversion rate, and accretion rate, respectively.

We adopt the equilibrium approach proposed by Grabowski, incorporating a temperature-dependent factor α to differentiate warm and cold cloud microphysics. Warm clouds dominate above 0°C and cold clouds below -20°C , with a linear interpolation for intermediate temperatures:

$$q_{vs} = \alpha q_{vw} + (1 - \alpha) q_{vi} \quad (5)$$

$$q_w = \alpha q_c, q_i = (1 - \alpha) q_c \quad (6)$$

$$q_r = \alpha q_p, q_s = (1 - \alpha) q_p \quad (7)$$

Here, q_{vs} represents the total vapor saturation, combining vapor saturation over water (q_{vw}) and ice (q_{vi}); q_w and q_i denote cloud water and ice, expressed as fractions of the cloud-ice mixture (q_c); q_r and q_s represent rain and snow, derived as fractions of the rain-snow mixture (q_p).

The transport equations for rain and snow processes include separate contributions from diffusional growth ($DIFF$), autoconversion ($AUTC$), and accretion ($ACCR$) rates:

$$DIFF = DIFF_r + DIFF_s \quad (8)$$

$$AUTC = AUTC_r + AUTC_s \quad (9)$$

$$ACCR = ACCR_r + ACCR_s \quad (10)$$

The terminal velocity v_p of precipitation is modeled as a weighted combination of rain (v_r) and snow (v_s) velocities, with typical values $v_r = -10\text{ m/s}$ for rain and $v_s = -2\text{ m/s}$:

$$v_p = \alpha v_r + (1 - \alpha) v_s \quad (11)$$

The saturation vapor mixing ratio q_{vs} combines contributions from vapor saturation over water and ice, weighted by α [Yau and Rogers(1996)]:

$$q_{vs} = \frac{380.16}{p} \left[\alpha \exp \left(\frac{17.67 \cdot T}{T + 243.50} \right) + (1 - \alpha) \exp \left(\frac{24.46 \cdot T}{T + 272.62} \right) \right] \quad (12)$$

Here, p represents the pressure, and T denotes the temperature. The saturation vapor is modeled as an exponential distribution for both liquid water and ice.

The diffusional growth rate $DIFF$ accounts for condensation and evaporation rates, integrating water and ice contributions [Dudhia(1989)], where β_r, β_s are phase-specific coefficients:

$$DIFF = \beta_r \cdot (\alpha \cdot q_{vs} - q_v)^+ + \beta_s \cdot ((1 - \alpha) \cdot q_{vs} - q_v)^+ \quad (13)$$

The autoconversion rate $AUTC$ describes cloud condensate aggregation into precipitation [Kessler(1995), Lin et al.(1983)]:

$$AUTC = \beta_r \cdot (\alpha \cdot q_c - 10^{-3})^+ + \beta_s \cdot e^{0.025T} \cdot ((1 - \alpha) \cdot q_c - 10^{-3})^+ \quad (14)$$

The accretion rate $ACCR$ models the collection of cloud condensate by precipitation particles [Morrison et al.(2015)]:

$$ACCR = q_c \cdot q_r \cdot (\beta_r \cdot \alpha^2 + \beta_s \cdot (1 - \alpha)^2) \quad (15)$$

4.2 Electrification

Based on the Reynolds-Brook theory of thunderstorm electrification [Latham and Miller(1965)], the fair-weather electric field (E) induces opposite charges on precipitation particles. Collisions between particles, influenced by their velocities and directions, result in partial charge neutralization and a residual net charge. Water droplet collisions generally coalesce without significant charge separation, while ice particle interactions are limited by brief contact times and low conductivity. Though water-ice and ice-riming collisions contribute, the inductive process alone is insufficient for thunderstorm-scale electric fields. This theory underpins the following mathematical model for electrification, with charge density (ρ) defined as:

$$\rho = k\alpha(1 - \alpha) (q_c^2 v_c - q_p^2 v_p) e^{-10q_v} \quad (16)$$

where k is a user-defined constant, v_c and v_p are their respective velocities of cloud-ice mixture and rain-snow mixture.

The threshold electric field (E_{tr}) required for lightning initiation depends on the altitude ($\rho_A(h)$) as defined by [Marshall et al.(1995)]:

$$E_{tr} = \pm 167 \rho_A(h) \quad \text{where} \quad \rho_A(h) = 1.208 \exp \left(\frac{-h}{8.4} \right) \quad (17)$$

Charge neutralization processes, occurring after a lightning discharge as described by [Barthe and Pinty(2007)], are governed by the following relationship:

$$\delta\rho = \begin{cases} \pm (|\rho| - \rho_{\text{excess}}), & \text{if } |\rho| > \rho_{\text{excess}} \\ 0, & \text{if } |\rho| \leq \rho_{\text{excess}} \end{cases} \quad (18)$$

Here, $\delta\rho$ represents the net charge change, and ρ_{excess} denotes the threshold for excess charge density. The total neutralized charge density, accounting for the collective contributions of lightning growth points, is expressed as:

$$\delta\rho_{\text{neut}} = \frac{1}{N} |(2\alpha - 1)q_c q_p| \sum_n \delta\rho \quad (19)$$

Finally, a suppression factor (S) is introduced to modulate lightning activity frequency as thunderstorms dissipate. This factor ensures consistent lightning activity during the lifecycle of thunderstorms:

$$S = \frac{1}{1 + k \cdot |\delta\rho_{\text{neut}}|} \quad (20)$$

4.3 Atmospheric Background

Our atmospheric background is based on the theory proposed by Hädrich et al. [Hädrich et al.(2020)]. Specifically, we assume that the atmosphere is initially electroneutral, with the charge density, denoted as ρ , being zero.

The isentropic exponent γ_{th} for the air-water mixture [Anderson(1990)] is calculated as a weighted average of the vapor-specific exponent γ_{vapor} and the air-specific exponent γ_{air} , as shown below:

$$\gamma_{\text{th}} = Y_{\text{vapor}}\gamma_{\text{vapor}} + (1 - Y_{\text{vapor}})\gamma_{\text{air}} \quad (21)$$

where Y_{vapor} represents the mass fraction of water vapor in the air. The values of γ_{air} and γ_{vapor} are taken as 1.4 and 1.33, respectively, based on standard thermodynamic properties of dry air and water vapor.

The atmospheric temperature profile [Atmosphere(1975)], $T(h)$, is modeled by a piecewise function that accounts for the lapse rate, including the effect of the inversion layer at a height h_1 . The temperature at a given altitude h is expressed as:

$$T(h) = \begin{cases} T_0 + \Gamma_0 h, & 0 \leq h \leq h_1 \\ T_0 + \Gamma_0 h_1 + \Gamma_1 (h - h_1), & h_1 \leq h \end{cases} \quad (22)$$

where T_0 is the base temperature at sea level, Γ_0 and Γ_1 represent the lapse rates in the lower and upper layers.

The atmospheric pressure profile, $p(h)$, is derived from the hydrostatic equation [Houze Jr(2014)], considering the effect of gravity and the ideal gas law. It is given by:

$$p(h) = p_0 \left(1 - \frac{\Gamma h}{T_0} \right)^{\frac{g}{R T_0}} \quad (23)$$

where p_0 is the pressure at sea level, g is the acceleration due to gravity, and R is the specific gas constant.

To model the thermodynamic properties of humid air, we calculate the average molar mass of the air-water mixture M_{th} . This is given by:

$$M_{th} = X_{\text{vapor}} M_{\text{water}} + (1 - X_{\text{vapor}}) M_{\text{air}} \quad (24)$$

where X_{vapor} is the mole fraction of water vapor, and M_{water} and M_{air} are the molar masses of water (18.02 g/mol) and dry air (28.96 g/mol), respectively.

The mass fraction of water vapor in the humid air, Y_{vapor} , is related to the mole fraction X_{vapor} by:

$$Y_{\text{vapor}} = X_{\text{vapor}} \frac{M_{\text{water}}}{M_{th}} \quad (25)$$

The temperature of the air in the atmosphere can also be related to pressure changes through the isentropic relation, which governs the temperature $T_{th}(h)$ at height h in terms of the pressure profile. This is given by:

$$T_{th}(h) = T_0 \left(\frac{p(h)}{p_0} \right)^{\frac{\gamma_{th}-1}{\gamma_{th}}} \quad (26)$$

Finally, the buoyancy force, which drives the upward movement of thundercloud, is calculated based on Archimedes' principle and Newton's second law. The buoyancy force $B(h)$ at height h is given by:

$$B(h) = g \left(\frac{M_{\text{air}}}{M_{th}} \frac{T_{th}(h)}{T_{\text{air}}(h)} - 1 \right) \quad (27)$$

4.4 Electrodynamics

The electrodynamic behavior of the atmosphere is governed by Maxwell's equations [Ma et al.(1998)], which define the relationships between the electric field \mathbf{E} , charge density ρ , and electric potential V . Gauss's law describes how the divergence of \mathbf{E} is proportional to ρ :

$$\nabla \cdot \mathbf{E} = \frac{\rho}{\epsilon_0} \quad (28)$$

where ϵ_0 is the permittivity of free space. The electric field is related to the potential V through:

$$\mathbf{E} = -\nabla V \quad (29)$$

indicating that \mathbf{E} points in the direction of decreasing potential. Together, these equations describe the electrostatic field and potential in regions with charge density.

To analyze the electric potential in the atmosphere, we solve the Poisson equation, a fundamental equation derived from Gauss’s law in electrostatics. This equation describes the simplified spatial variation of the potential V due to charge density ρ [Kim and Lin(2007)]:

$$\nabla^2 V = -4\pi\rho \quad (30)$$

For simulating lightning discharges, the Dielectric Breakdown Model (DBM) is employed[Niemeyer et al.(1984)]. The probability of a discharge at a specific point i depends on the electric potential V_i , expressed as:

$$p_i = \frac{(V_i)^\eta}{\sum_{j=1}^n (V_j)^\eta} \quad (31)$$

Here, η is a parameter controlling the spatial concentration of the discharge[Kim and Lin(2007)]. Larger values of η bias the discharge toward regions of higher potential, while smaller values allow for more diffusive propagation. The sum in the denominator normalizes the probabilities, ensuring that the total probability across all potential locations is unity. This formulation effectively models lightning channel growth, as discharges preferentially propagate along paths with elevated electric potential.

4.5 Fluid Dynamics

The motion of atmospheric fluids is described by the Navier-Stokes equations, which represent the conservation of momentum in a fluid medium [Wendt(2008)]. These equations capture the effects of inertial forces, pressure gradients, viscosity, and external forces:

$$\frac{\partial(\rho\mathbf{u})}{\partial t} + \nabla \cdot (\rho\mathbf{u}\mathbf{u}) = -\nabla p + \rho(\mu\nabla^2\mathbf{u} + \mathbf{b} + \mathbf{f}), \quad \nabla \cdot \mathbf{u} = 0 \quad (32)$$

Here, ρ is the fluid density, \mathbf{u} the velocity field, p the pressure, μ the dynamic viscosity, \mathbf{b} the body force (e.g., gravity), and \mathbf{f} external forces. The incompressibility condition $\nabla \cdot \mathbf{u} = 0$ ensures mass conservation for incompressible flows.

For efficient large-scale atmospheric simulations, we employ the compact Poisson filter method[Rabbani et al.(2022)]. This GPU-friendly solver converts iterative Jacobi steps into a single convolution operation, enabling scalable fluid simulations with controllable accuracy and effective boundary condition handling.

The method solves for a scalar field Φ , which represents the field to be solved in the Poisson equation during the pressure projection. Using the symmetric Poisson kernel K , the solution is expressed as:

$$K * \Phi = \sum_{i=0}^r \mathbf{e}_i *_x (\mathbf{e}_i *_y (\mathbf{e}_i *_z \Phi)) \quad (33)$$

Here, \mathbf{e}_i are the eigenvectors of K , r is the matrix rank, and $*$ denotes convolution along spatial dimensions (x , y , and z).

5 ALGORITHMICS

Algorithm 1 Thunderstorm Development Algorithm.

```

1: Input: Current MCS state  $(\theta, p, \rho, u, q_v, q_c, q_p)$ .
2: Output: Updated MCS state.
3: procedure
4:    $\theta, p, \rho \leftarrow$  Update atmospheric background conditions           Eqs.(22–23)
5:    $u \leftarrow$  Advect and diffuse velocity field
6:    $b \leftarrow$  Compute thermal buoyancy                               Eq.(27)
7:    $u \leftarrow u + b + f_w + f_v$     $\triangleright$  Apply buoyancy, wind, vorticity confinement
8:    $q_v, q_c, q_p \leftarrow$  Advect hydrometeor quantities
9:    $u \leftarrow$  Pressure projection using the compact poisson filter     Eq.(33)
10:   $q_v, q_c, q_p, \theta, \rho \leftarrow$  Thundercloud microphysics update   Eqs.(1–15)
11:  if  $S \cdot \rho > E_{tr}$  then            $\triangleright$  Electrification process       Eq.(16–18)
12:     $V, \rho_{neut} \leftarrow$  lightning discharge                       Eqs.(30–31),(19)
13:     $S \cdot \rho \leftarrow$  Apply lightning neutralization               Eq.(20)
14:  end if
15: end procedure

```

The theory discussed in the previous section is implemented as a numerical procedure outlined in Algorithm 1. Figure 1 illustrates the interrelationships governing thunderstorm development. We begin by detailing our procedure for modeling the life cycle of a Mesoscale Convective System (MCS). Subsequently, we describe the dynamics of lightning channel growth, which occurs when the electric field threshold is exceeded. Additionally, we present a lightweight parameter toolset designed to facilitate interactive simulation.

5.1 Mesoscale Convective System Cycle

The input fields for the MCS system, depicted in Figure 3, serve as the foundation for initializing state variables, including potential temperature (θ), pressure (p), charge density (ρ), velocity field (u), and hydrometeor quantities (q_v , q_c , q_p). The solver updates these variables iteratively, producing an output that represents the evolved state of the MCS, incorporating changes driven by thundercloud microphysics and the electrification processes.

The procedure begins by updating the atmospheric background conditions, through governing equations (Eqs. 22–23).

The velocity field is then advected and diffused. Thermal buoyancy is computed (Eq. 27) and integrated into the velocity field, alongside contributions from wind and vorticity confinement forces.

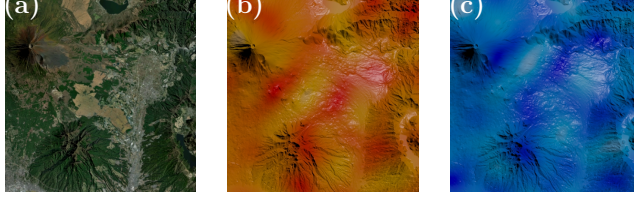


Figure 3: Different types of sources used as input for our MCS solver, temperature and vapor field are sampled from perlin noise patterns. (a) Height field derived from satellite data, (b) ground temperature distribution, (c) vapor field distribution.

Hydrometeor quantities (q_v , q_c , q_p) are transported according to the evolving velocity field through advection. Pressure projection, using the compact Poisson filter (Eq. 33), is applied to ensure stability and enforce flow field divergence constraints. Cloud microphysics are subsequently updated, incorporating processes such as condensation, evaporation, and precipitation, governed by parameterized equations (Eqs. 1–15).

Boundary conditions for the vapor field (q_v) include periodic boundaries in the horizontal directions and a Dirichlet condition at the top. For temperature (θ), Dirichlet conditions apply in the horizontal and top directions, with a Neumann condition at the bottom.

Electrification is initiated when the charge density, modulated by the suppress factor ($S \cdot \rho$), exceeds the electric field threshold (E_{tr} , Eqs. 16–18). This triggers lightning discharges, which are detailed in the next subsection. Following lightning activity, the neutralized charge density (ρ_{neut} , Eqs. 30–31, 19) is updated, redistributing charge density ($S \cdot \rho$, Eq. 20). The suppress factor is recalibrated to reflect the diminished likelihood of subsequent lightning events as the system dissipates.

5.2 Lightning Channel Growth

The growth of the lightning channel begins at a trigger point, which is randomly selected from locations where the electric field exceeds the threshold. The spatial domain for modeling the lightning channel growth is typically represented at a subgrid scale within the thunderstorm model, using a coarser grid size. [Mansell et al.(2002)] This is because the lightning channel is much more sparse compared to the broader thundercloud structure, and it only appears in a limited region of the sky.

Drawing inspiration from the DBM model proposed by [Kim and Lin(2007)], the lightning channel growth is terminated once it reaches a positive charge object. This approach provides greater flexibility in controlling the final structure of the lightning channel, while also improving computational efficiency.

For cloud-to-ground (CG) lightning, a positive charge configuration is assumed to exist on the ground, with the electric potential set to one. In contrast,

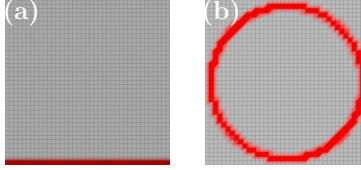


Figure 4: Initial charge configurations for different types of lightning. (a) CG Lightning, (b) IC Lightning. Red regions represent areas where the electric potential is equal to 1.

for intracloud (IC) lightning, a radial positive charge distribution is established within the boundary of the lightning solving grid, as shown in Figure 4.

The evolution of the lightning channel is modeled by solving the Poisson equation (Eq. 30), using the Gauss-Seidel Successive Overrelaxation (SOR) method. The solution is performed on a grid, and then the results are converted from grid points to geometrical points. To achieve a more natural branching structure, we apply a dithering technique to the points.

Additionally, we employ a custom edge transport method to differentiate point groupings, allowing the model to separately control the widths of return strokes and dart leaders. Finally, this process yields the lightning geometry for the current simulation frame, which is then prepared for rendering.

6 VISUALIZATION

Our tool is implemented as a HDA (Houdini Digital Asset) using Houdini 20.0.625's microsolver framework with OpenCL for GPU acceleration. The hardware setup includes NVIDIA® GeForce® RTX 3060 Ti GPU, 13th Gen Intel® Core™ i5-13600KF processor, and 32GB of RAM.

The simulation results demonstrate various thunderstorm and lightning phenomena, integrated with scenarios inspired by real-world weather events. As shown in Table ??, we summarize the lightweight parameter set used for the scenes presented in this section. All renders are produced using Houdini's native volumetric rendering engine to ensure high-quality visual outputs.

6.1 Thunderstorms Variation

We simulate four common types of thunderstorms that occur within a mesoscale convective system (MCS), capturing their distinctive characteristics and dynamic behaviors:

- **Single Cell:** This is the simplest form of thunderstorm, typically short-lived and consisting of a single updraft and downdraft cycle. It often forms in isolated conditions and usually dissipates within an hour.

- **Multicell:** Multicell thunderstorms are composed of multiple convective cells at various stages of their life cycle. These storms exhibit greater longevity and intensity compared to single cells, as new cells continuously form along the gust front of the system.
- **Squall Line:** A squall line is a collection of thunderstorms that align into a long, narrow band, often stretching hundreds of miles. This type of storm is typically associated with intense winds, heavy rainfall, and the characteristic "shelf cloud" feature that marks the leading edge of the gust front.
- **Supercell:** The supercell is the most intense and organized type of thunderstorm, characterized by a rotating updraft known as a mesocyclone. These storms are capable of producing severe weather phenomena, including large hail, damaging winds, and tornadoes.

These simulated variations allow us to explore the diverse behaviors and impacts of thunderstorms within an MCS. The visual comparison of these thunderstorm types is presented in Figure ??, highlighting their structural differences and unique features.

6.2 Severe Weather Phenomena

To explore the impact of thunderstorms in real-world scenarios, we reference severe weather events in geographically diverse locations. These events illustrate the variability and intensity of thunderstorms in different environments:

These events serve as the basis for our simulations, showcasing the capability of our model to replicate the diverse and complex phenomena associated with severe weather. The corresponding visualizations are presented in Figure ??.

7 VALIDATION

We follow the evaluation methods in [Shen et al.(2020)] and [Cesana et al.(2019)], tracking altitude-based quantitative data to analyze cloud behavior across atmospheric layers. Results are shown in Figure ??.

Following the methodology in [Herrera et al.(2021)], we analyze the temporal evolution of four storm types: single cell, multicell, squall line, and supercell. Cloud coverage evolution reveals dynamic distribution changes, while temperature evolution highlights thermal dynamics and energy exchanges.

Following the evaluation method in [Formenton et al.(2013)], We analyze the lightning flash rate evolution to capture thunderstorm electrical activity. The flash rate rises during storm development and falls to zero as it dissipates, reflecting the storm lifecycle and charge dynamics.

We specifically selected four regions frequently studied in thunderstorms meteorology [Uman(2001), Harris and Carvalho(2018)] to validate our model by comparing its simulation results with real-world weather data. Our focus

includes cloud cover dynamics, temperature trends, and relative humidity variations.

Figure ?? illustrates this comparison across Florida, New Mexico, Japan, and California, showcasing the model’s capability to capture diverse climatic behaviors and atmospheric dynamics.

8 CONCLUSION AND FUTURE WORK

We have developed a comprehensive framework for simulating atmospheric phenomena during thunderstorms, focusing on thundercloud development, dissipation, and lightning generation through cloud electrification processes. This framework integrates a Grabowski-style extended warm cloud microphysics scheme with hydrometeor electrification processes to ensure the consistent coupling of cloud formation and lightning dynamics. Additionally, we incorporated a compact Poisson filter into the fluid dynamics solver to achieve efficient, high-performance simulations with a balance of stability and computational accuracy. The model simulates key atmospheric quantities, including microphysical properties such as vapor, cloud water, ice, and precipitated rain and snow, as well as electrodynamic properties like static charge distribution and lightning flashes. Our framework reproduces various thundercloud types, including single-cell, multicell, squall line, supercell, and atmospheric river formations, and simulates lightning dynamics using the Dielectric Breakdown Model (DBM), capturing both cloud-to-ground and intra-cloud lightning. Validation against real-world weather data demonstrates the model’s accuracy in simulating cloud structure, temperature evolution, cloud coverage, relative humidity, and lightning flash rates, with results benchmarked against national weather services and observed lightning activity.

Future work will focus on expanding the framework to incorporate advanced atmospheric concepts and support a broader range of thunderstorm and lightning phenomena. Enhancements to thunderstorm microphysics, such as more detailed electrification processes and turbulence modeling, will improve the realism of lightning generation. The framework will also be extended to simulate additional thunderstorm types, including Mesoscale Convective Complex (MCC), Mesoscale Convective Vortex (MCV), and derechos, broadening its coverage of mesoscale systems. Furthermore, new lightning types such as anvil crawlers, bolts from the blue, and sheet lightning will be introduced, requiring refined electric field and branching models. Finally, scalability and real-time performance will be improved by leveraging advanced numerical techniques and hardware optimizations, enabling more detailed and interactive simulations.

REFERENCES

[Amador Herrera et al.(2024)] Jorge Alejandro Amador Herrera, Jonathan Klein, Daoming Liu, Wojtek Pabubicki, Sören Pirk, and Dominik L Michels.

2024. Cyclogenesis: Simulating Hurricanes and Tornadoes. *ACM Transactions on Graphics (TOG)* 43, 4 (2024), 1–16.
- [Anderson(1990)] John David Anderson. 1990. Modern compressible flow: with historical perspective. (*No Title*) (1990).
- [Atmosphere(1975)] Standard Atmosphere. 1975. International organization for standardization. *ISO 2533* (1975), 1975.
- [Barthe and Pinty(2007)] Christelle Barthe and Jean-Pierre Pinty. 2007. Simulation of a supercellular storm using a three-dimensional mesoscale model with an explicit lightning flash scheme. *Journal of Geophysical Research: Atmospheres* 112, D6 (2007).
- [Cesana et al.(2019)] Grégory Cesana, Anthony D Del Genio, and Hélène Chepfer. 2019. The cumulus and stratocumulus CloudSat-CALIPSO dataset (CASCAD). *Earth System Science Data* 11, 4 (2019), 1745–1764.
- [Dudhia(1989)] Jimmy Dudhia. 1989. Numerical study of convection observed during the winter monsoon experiment using a mesoscale two-dimensional model. *Journal of Atmospheric Sciences* 46, 20 (1989), 3077–3107.
- [Ferreira Barbosa et al.(2015)] Charles Welton Ferreira Barbosa, Yoshinori Dobashi, and Tsuyoshi Yamamoto. 2015. Adaptive cloud simulation using position based fluids. *Computer Animation and Virtual Worlds* 26, 3-4 (2015), 367–375.
- [Formenton et al.(2013)] M Formenton, G Panegrossi, D Casella, S Dietrich, A Mugnai, P Sanò, F Di Paola, H-D Betz, C Price, and Yoav Yair. 2013. Using a cloud electrification model to study relationships between lightning activity and cloud microphysical structure. *Natural Hazards and Earth System Sciences* 13, 4 (2013), 1085–1104.
- [Garcia-Dorado et al.(2017)] Ignacio Garcia-Dorado, Daniel G Aliaga, Saiprasanth Bhalachandran, Paul Schmid, and Dev Niyogi. 2017. Fast weather simulation for inverse procedural design of 3d urban models. *ACM Transactions on Graphics (TOG)* 36, 2 (2017), 1–19.
- [Goswami and Neyret(2017)] Prashant Goswami and Fabrice Neyret. 2017. Real-time landscape-size convective clouds simulation and rendering. In *VRIPHYS 2017-13th Workshop on Virtual Reality Interaction and Physiscal Simulation*.
- [Grabowski(1998)] Wojciech W Grabowski. 1998. Toward cloud resolving modeling of large-scale tropical circulations: A simple cloud microphysics parameterization. *Journal of the Atmospheric Sciences* 55, 21 (1998), 3283–3298.

- [Hädrich et al.(2020)] Torsten Hädrich, Miłosz Makowski, Wojtek Pałubicki, Daniel T Banuti, Sören Pirk, and Dominik L Michels. 2020. Stormscapes: Simulating cloud dynamics in the now. *ACM Transactions on Graphics (TOG)* 39, 6 (2020), 1–16.
- [Harris and Carvalho(2018)] Sarah M Harris and Leila MV Carvalho. 2018. Characteristics of southern California atmospheric rivers. *Theoretical and applied climatology* 132 (2018), 965–981.
- [Herrera et al.(2021)] Jorge Alejandro Amador Herrera, Torsten Hädrich, Wojtek Pałubicki, Daniel T Banuti, Sören Pirk, and Dominik L Michels. 2021. Weatherscapes: Nowcasting heat transfer and water continuity. *ACM Transactions on Graphics (TOG)* 40, 6 (2021), 1–19.
- [Houze Jr(2014)] Robert A Houze Jr. 2014. *Cloud dynamics*. Academic press.
- [Kessler(1969)] Edwin Kessler. 1969. On the distribution and continuity of water substance in atmospheric circulations. In *On the distribution and continuity of water substance in atmospheric circulations*. Springer, 1–84.
- [Kessler(1995)] Edwin Kessler. 1995. On the continuity and distribution of water substance in atmospheric circulations. *Atmospheric research* 38, 1-4 (1995), 109–145.
- [Kim and Lin(2007)] Theodore Kim and Ming C Lin. 2007. Fast animation of lightning using an adaptive mesh. *IEEE Transactions on Visualization and Computer Graphics* 13, 2 (2007), 390–402.
- [Lastic et al.(2022)] Maud Lastic, Damien Rohmer, Guillaume Cordonnier, Claude Jaupart, Fabrice Neyret, and Marie-Paule Cani. 2022. Interactive simulation of plume and pyroclastic volcanic ejections. *Proceedings of the ACM on Computer Graphics and Interactive Techniques* 5, 1 (2022), 1–15.
- [Latham and Miller(1965)] J Latham and AH Miller. 1965. The role of ice specimen geometry and impact velocity in the Reynolds-Brook theory of thunderstorm electrification. *Journal of Atmospheric Sciences* 22, 5 (1965), 505–508.
- [Lin et al.(1983)] Yuh-Lang Lin, Richard D Farley, and Harold D Orville. 1983. Bulk parameterization of the snow field in a cloud model. *Journal of Applied Meteorology and climatology* 22, 6 (1983), 1065–1092.
- [Ma et al.(1998)] Zhaofeng Ma, CL Croskey, and LC Hale. 1998. The electrodynamic responses of the atmosphere and ionosphere to the lightning discharge. *Journal of atmospheric and solar-terrestrial physics* 60, 7-9 (1998), 845–861.

- [Mansell et al.(2002)] Edward R Mansell, Donald R MacGorman, Conrad L Ziegler, and Jerry M Straka. 2002. Simulated three-dimensional branched lightning in a numerical thunderstorm model. *Journal of Geophysical Research: Atmospheres* 107, D9 (2002), ACL-2.
- [Mansell et al.(2010)] Edward R Mansell, Conrad L Ziegler, and Eric C Bruning. 2010. Simulated electrification of a small thunderstorm with two-moment bulk microphysics. *Journal of the Atmospheric Sciences* 67, 1 (2010), 171–194.
- [Marshall et al.(1995)] Thomas C Marshall, Michael P McCarthy, and W David Rust. 1995. Electric field magnitudes and lightning initiation in thunderstorms. *Journal of Geophysical Research: Atmospheres* 100, D4 (1995), 7097–7103.
- [Miyazaki et al.(2002)] Ryo Miyazaki, Yoshinori Dobashi, and Tomoyuki Nishita. 2002. Simulation of Cumuliform Clouds Based on Computational Fluid Dynamics.. In *Eurographics (Short Presentations)*.
- [Morrison et al.(2015)] Hugh Morrison, Jason A Milbrandt, George H Bryan, Kyoko Ikeda, Sarah A Tessendorf, and Gregory Thompson. 2015. Parameterization of cloud microphysics based on the prediction of bulk ice particle properties. Part II: Case study comparisons with observations and other schemes. *Journal of the Atmospheric Sciences* 72, 1 (2015), 312–339.
- [Niemeyer et al.(1984)] Lucian Niemeyer, Luciano Pietronero, and Hans J Wiesmann. 1984. Fractal dimension of dielectric breakdown. *Physical Review Letters* 52, 12 (1984), 1033.
- [Pretorius et al.(2024)] Pieter C Pretorius, James Gain, Maud Lastic, Guillaume Cordonnier, Jiong Chen, Damien Rohmer, and M-P Cani. 2024. Volcanic Skies: coupling explosive eruptions with atmospheric simulation to create consistent skies. In *Computer Graphics Forum*, Vol. 43. Wiley Online Library, e15034.
- [Rabbani et al.(2022)] Amir Hossein Rabbani, Jean-Philippe Guertin, Damien Rioux-Lavoie, Arnaud Schoentgen, Kaitai Tong, Alexandre Sirois-Vigneux, and Derek Nowrouzezahrai. 2022. Compact Poisson Filters for Fast Fluid Simulation. In *ACM SIGGRAPH 2022 Conference Proceedings*. 1–9.
- [Reed and Wyvill(1994)] Todd Reed and Brian Wyvill. 1994. Visual simulation of lightning. In *Proceedings of the 21st annual conference on Computer graphics and interactive techniques*. 359–364.
- [Shen et al.(2020)] Zhaoyi Shen, Kyle G Pressel, Zhihong Tan, and Tapio Schneider. 2020. Statistically steady state large-eddy simulations forced by an idealized GCM: 1. Forcing framework and simulation characteristics. *Journal of Advances in Modeling Earth Systems* 12, 2 (2020), e2019MS001814.

- [Solomon et al.(2005)] R Solomon, CM Medaglia, C Adamo, S Dietrich, A Mugnai, and Ugo Biader Ceipidor. 2005. An explicit microphysics thunderstorm model. *International Journal of Modelling and Simulation* 25, 2 (2005), 112–118.
- [Stam(1999)] Jos Stam. 1999. Stable fluids. In *Proceedings of the 26th Annual Conference on Computer Graphics and Interactive Techniques (SIGGRAPH '99)*. ACM Press/Addison-Wesley Publishing Co., USA, 121–128. <https://doi.org/10.1145/311535.311548>
- [Uman(2001)] Martin A Uman. 2001. *The lightning discharge*. Courier Corporation.
- [Vimont et al.(2020)] Ulysse Vimont, James Gain, Maud Lastic, Guillaume Cordonnier, Babatunde Abiodun, and Marie-Paule Cani. 2020. Interactive Meso-scale Simulation of Skyscapes. In *Computer Graphics Forum*, Vol. 39. Wiley Online Library, 585–596.
- [Webanck et al.(2018)] Antoine Webanck, Yann Cortial, Eric Guérin, and Eric Galin. 2018. Procedural cloudscares. In *Computer Graphics Forum*, Vol. 37. Wiley Online Library, 431–442.
- [Wendt(2008)] John F Wendt. 2008. *Computational fluid dynamics: an introduction*. Springer Science & Business Media.
- [Wu et al.(2023)] Kenan Wu, Tianwen Wei, Jinlong Yuan, Haiyun Xia, Xin Huang, Gaopeng Lu, Yunpeng Zhang, Feifan Liu, Baoyou Zhu, and Weidong Ding. 2023. Thundercloud structures detected and analyzed based on coherent Doppler wind lidar. *Atmospheric Measurement Techniques Discussions* 2023 (2023), 1–22.
- [Yau and Rogers(1996)] Man Kong Yau and Roddy Rhodes Rogers. 1996. *A short course in cloud physics*. Elsevier.
- [Yun et al.(2017)] Jeongsu Yun, Myungbae Son, Byungyoon Choi, Theodore Kim, and Sung-Eui Yoon. 2017. Physically inspired, interactive lightning generation. *Computer Animation and Virtual Worlds* 28, 3-4 (2017), e1760.
- [Zhang et al.(2020)] Zili Zhang, Yunfei Li, Bailin Yang, Frederick WB Li, and Xiaohui Liang. 2020. Target-driven cloud evolution using position-based fluids. *Computer Animation and Virtual Worlds* 31, 6 (2020), e1937.